Disruption of endoplasmic reticulum structure and integrity in lipotoxic cell death

Nica M. Borradaile,[*] Xianlin Han,[†] Jeffrey D. Harp,[*] Sarah E. Gale,[*] Daniel S. Ory,[*] and Jean E. Schaffer[1,*]

Center for Cardiovascular Research, Division of Cardiology,[*] and Division of Bioorganic Chemistry,[†] Department of Internal Medicine, Washington University School of Medicine, St. Louis, MO 63110

Abstract **Cell dysfunction and death induced by lipid accumulation in nonadipose tissues, or lipotoxicity, may contribute to the pathogenesis of obesity and type 2 diabetes. However, the mechanisms leading to lipotoxic cell death are poorly understood. We recently reported that, in Chinese hamster ovary (CHO) cells and in H9c2 cardiomyoblasts, lipid overload induced by incubation with 500 μM palmitate leads to intracellular accumulation of reactive oxygen species, which subsequently induce endoplasmic reticulum (ER) stress and cell death. Here, we show that palmitate also impairs ER function through a more direct mechanism. Palmitate was rapidly incorporated into saturated phospholipid and triglyceride species in microsomal membranes of CHO cells. The resulting membrane remodeling was associated with dramatic dilatation of the ER and redistribution of protein-folding chaperones to the cytosol within 5 h, indicating compromised ER membrane integrity. Increasing β-oxidation, through the activation of AMP-activated protein kinase, decreased palmitate incorporation into microsomes, decreased the escape of chaperones to the cytosol, and decreased subsequent caspase activation and cell death. Thus, palmitate rapidly increases the saturated lipid content of the ER, leading to compromised ER morphology and integrity, suggesting that impairment of the structure and function of this organelle is involved in the cellular response to fatty acid overload.—** Borradaile, N. M., X. Han, J. D. Harp, S. E. Gale, D. S. Ory, and J. E. Schaffer. **Disruption of endoplasmic reticulum structure and integrity in lipotoxic cell death. *J. Lipid Res.* 2006.** 47: **2726–2737.**

Supplementary key words palmitate • fatty acid • lipotoxicity • lipid synthesis

Increased serum triacylglycerol (TAG) and NEFA levels, associated with obesity and type 2 diabetes, contribute to lipid accumulation in many nonadipose tissues. Through the process of lipotoxicity, this inappropriate accumulation of excess lipid can lead to cellular dysfunction and cell death (1). For example, evidence from rodent models strongly implicates cardiac accumulation of lipid in the genesis of heart failure in diabetes. TAG accumulation in cardiomyocytes of leptin- or leptin receptor-deficient obese diabetic animal models is associated with cardiomyocyte apoptosis (2) and contractile dysfunction (2–4). Consistent with this apparent cardiac lipotoxicity, cardiomyocyte-specific increases in FA uptake in mice with cardiac-restricted overexpression of long-chain acyl-CoA synthetase 1, lipoprotein lipase, or fatty acid transport protein 1 are sufficient to cause cardiomyocyte dysfunction and/or death that lead to left ventricular dysfunction (5–7).

Studies using cultured cells to model the lipotoxic response have helped elucidate the mechanisms involved in the response to FA overload. Long-chain saturated fatty acids, such as palmitate, induce cell death in a variety of cell types, including cardiomyocytes (8). In general, palmitate-induced cell death is characterized by markers of apoptosis, including cytochrome c release, caspase activation, and DNA fragmentation. Although relatively few studies have focused on mechanisms of palmitate-induced cell death in cardiomyocytes, recent evidence obtained using primary cardiomyocyte cultures from embryonic chicks and neonatal rats suggests that incubation with palmitate is associated with the loss of mitochondrial membrane potential, mitochondrial swelling, and cytochrome c release (9–11). These events may be initiated via several mechanisms, including decreased synthesis of the signature mitochondrial membrane phospholipid, cardiolipin (11), increased ceramide synthesis (9, 12), and increased generation of reactive oxygen species (ROS) (13, 14). However, the induction of apoptosis by both ceramide and oxidative stress requires a flux of calcium ions from the endoplasmic reticulum (ER) to the mitochondria (15, 16), and depletion of these calcium stores can impair normal protein-folding functions, leading to ER stress (17,

Manuscript received 10 July 2006 and in revised form 25 August 2006.
Published, JLR Papers in Press, September 7, 2006.
DOI 10.1194/jlr.M600299-JLR200

Abbreviations: AICAr, 5-aminoimidazole-4-carboxamide-1-β-4-ribofuranoside; AMPK, AMP-activated protein kinase; ER, endoplasmic reticulum; GRP78, glucose-regulated protein 78; PC, phosphatidylcholine; PDI, protein disulfide isomerase; ROS, reactive oxygen species; SCD1, stearoyl-coenzyme A desaturase 1; TAG, triacylglycerol.

[1] To whom correspondence should be addressed.
e-mail: jschaff@wustl.edu

18). Consistent with this concept, we and others recently showed that palmitate overload rapidly induces ER stress in pancreatic β-cells (19), hepatocytes (20), and cardiomyoblasts (14). Furthermore, our studies revealed that palmitate-induced ER stress was mediated, in part, through the generation of ROS (14).

Several observations indicate that palmitate may also act more directly at the level of the ER to initiate a lipotoxic response. In vitro evidence suggests that palmitoyl-CoA facilitates ER fission (21) and that the acyl chains of lipids directly affect the fusion/fission events of membranes (22, 23). Furthermore, incorporation of saturated fatty acyl chains into membrane phospholipids can induce detrimental stiffening of cellular membranes (24–26). Here, we demonstrate that, in CHO cells and H9c2 cardiomyoblasts, the rapid induction of ER stress in the presence of palmitate is associated with the rapid incorporation of this fatty acid into lipid components of the rough ER and subsequent compromise of rough ER structure and integrity. Although previous studies indicate that palmitate-induced intracellular responses converge on the mitochondria, eventually resulting in the release of cytochrome c into the cytosol and apoptotic cell death, our studies suggest that the ER may play an important proximal role in FA-induced cytotoxicity.

MATERIALS AND METHODS

Cell culture and chemicals

CHO-K1 (CHO) cells (American Type Culture Collection) and stearoyl-coenzyme A desaturase 1 (SCD1)-overexpressing CHO cells (27) were maintained in high-glucose (4.5 mg/ml) DMEM and Ham's F-12 nutrient mixture (1:1), with 5% FBS, as described (27). H9c2 rat cardiomyoblasts (American Type Culture Collection) were maintained in high-glucose DMEM with 10% FBS, as described (14). For experiments, all CHO and H9c2 cell lines (90% confluent) were incubated in CHO cell growth medium supplemented with palmitate (500 μM) or oleate (500 μM) (Nu-Chek Prep) complexed to BSA at a 2:1 molar ratio, prepared as described previously (13). 5-Aminoimidazole-4-carboxamide-1-β-4-ribofuranoside (AICAr) was from Calbiochem; etomoxir, H_2O_2, α-tocopherol (vitamin E), thapsigargin, and DMSO were from Sigma.

Subcellular distribution of radiolabeled palmitate

CHO cells were incubated for 1 h with [9,10-^{3}H]palmitate (Perkin-Elmer), [9,10-^{3}H]oleate (Perkin-Elmer), or [9,10-^{3}H]2-bromopalmitate (American Radiochemicals) at a specific activity of 10 μCi/mmol. Crude mitochondria, cytosol, smooth microsomes, and rough microsomes were isolated by homogenization and sequential centrifugation, as described previously (28). Radioactivity in each fraction was measured using a Beckman LS 6000IC scintillation counter and normalized to the total protein in each fraction (BCA Protein Assay; Pierce). The relative purity of the isolated fractions was assessed by immunoblotting using rabbit polyclonal antibodies against histone H1 (Stressgen), long-chain acyl-CoA dehydrogenase [a gift from A. Strauss (29)], and p63 [a gift from J. Rohrer (30)].

Lipid composition of rough microsomes

CHO cells were incubated for 1 h in the absence or presence of 500 μM [7,7,8,8-^{2}H]palmitate (Cambridge Isotope). Rough microsomes were isolated as described above. Lipids were extracted and lipid species were identified and quantitated by electrospray ionization mass spectrometry (31, 32). The mass levels of phosphatidylethanolamine were not determined in this study.

Electron microscopy

CHO cells were harvested, fixed with 2.5% glutaraldehyde in 0.1 M sodium cacodylate buffer, postfixed in 1.25% osmium tetroxide, and stained with 4% aqueous uranyl acetate. Embedded tissue was then thin-sectioned and viewed on a Zeiss 902 electron microscope. Glutaraldehyde, osmium tetroxide, and uranyl acetate were from Electron Microscopy Sciences.

Subcellular fractionation and immunoblotting

Crude cytosolic and membrane/organelle fractions were isolated from CHO cells by sequential detergent extraction using ProteoExtract reagents from Calbiochem (33). Based on our preliminary assessment of the distribution of marker proteins, an alternative method of homogenization and sequential centrifugation (34) was required to isolate cytosolic and crude microsomal fractions from H9c2 cells. Glucose-regulated protein 78 (GRP78) and protein disulfide isomerase (PDI) in 7.5–20 μg of protein from each subcellular fraction were detected using rabbit polyclonal antibodies (Stressgen). Cytochrome c in 40–80 μg of protein from crude mitochondrial and cytosolic fractions, isolated by sequential centrifugation, was detected using a monoclonal antibody (BD Biosciences).

ER calcium depletion

Palmitate-induced depletion of thapsigargin-sensitive calcium stores was assessed using the Fluo-4 NW calcium assay kit (Molecular Probes, Invitrogen) in a 96-well plate format, according to the manufacturer's protocol. After incubation with palmitate, cells were loaded with Fluo-4 AM in the presence of 2.5 mM probenicid. Thapsigargin (1 μM) or vehicle (DMSO) was added immediately, and fluorescence at 2 min was measured using a Hidex plate reader (excitation at 485 nm and emission at 535 nm). Data were expressed as fluorescent increments (change in fluorescence) upon addition of thapsigargin.

Mitochondrial staining

Depolarization of mitochondria was assessed using the potential-dependent dye, JC-1 (Molecular Probes, Invitrogen). CHO cells incubated for up to 5 h with 500 μM palmitate or 2.5 mM H_2O_2 were stained with 7.5 μM JC-1 at 37°C, according to the manufacturer's protocol. Mean red and green fluorescence were determined by flow cytometry (10^4 cells/sample) for subsequent calculation of mean FL2/FL1 ratios.

The presence of intact mitochondria was assessed using MitoTracker Green FM (Molecular Probes, Invitrogen). CHO cells incubated for up to 18 h with 500 μM palmitate or 2.5 mM H_2O_2 were stained for 30 min with 20 nM MitoTracker Green FM at 37°C, according to the manufacturer's protocol. Mean fluorescence was determined by flow cytometry (10^4 cells/sample).

Caspase activation and cell death

Activation of caspases-3 and -7 was determined by immunoblotting of cytosolic (40 μg of protein) and microsomal (70 μg of protein) fractions from H9c2 cells incubated for up to 24 h with various treatments. Rabbit polyclonal antibodies were used to simultaneously detect both pro- (inactive) and cleaved (active) forms of each caspase (Cell Signaling Technologies). Cell death was assessed by membrane permeability to propidium iodide, as

described previously (13). Briefly, CHO and H9c2 cells incubated for 24–48 h with various treatments were harvested by trypsinization and stained with 1 μM propidium iodide. The percentage of propidium iodide-positive cells was determined by flow cytometry (10^4 cells/sample).

RESULTS

Palmitate is rapidly incorporated into saturated phospholipid and triglyceride species in the rough ER

Previous studies have identified the ER as a target of palmitate-induced lipotoxicity downstream of the generation of ROS (14). To test the hypothesis that palmitate may also impair ER function more directly through its rapid incorporation into the ER membrane, we determined the subcellular distribution of palmitate within 1 h of exposure to a lipotoxic dose. CHO cells were incubated with 500 μM palmitate containing a trace amount of [^{3}H]palmitate. Subsequent subcellular fractionation revealed that the bulk of the label was distributed between the crude mitochondrial fraction (58.00 ± 0.03%) and the rough microsomal fraction (22.90 ± 0.03%) (**Fig. 1A**). Although a significant proportion of [^{3}H]palmitate was associated with the relatively pure rough microsomal fraction, composed predominantly of rough ER, the crude mitochondria were contaminated with rough microsomes (Fig. 1C), indicating that the calculated percentage distribution actually underestimates the incorporation of palmitate into the rough ER. Similar distributions were observed upon labeling of CHO cells with oleate and upon labeling of CHO cells overexpressing SCD1 with palmitate. These SCD1-overexpressing cells have an increased capacity to introduce double bonds into palmitate by virtue of increased SCD1 activity (27). Thus, exogenous saturated and unsaturated FAs are channeled quickly to the ER as well as to the mitochondria. This distribution is independent of lipotoxicity, which occurs in CHO cells treated with palmitate but not in CHO cells treated with oleate or SCD1-overexpressing cells treated with palmitate (27).

To determine whether modulating β-oxidation could alter the distribution observed with 500 μM palmitate, the same experiment was conducted in the presence of either etomoxir (an inhibitor of carnitine palmitoyl transferase 1) or AICAr [an activator of AMP-activated protein kinase (AMPK)] (Fig. 1A). These compounds were used at doses established previously to effectively inhibit or increase β-oxidation (35, 36). Etomoxir did not alter the subcellular distribution of [^{3}H]palmitate within 1 h, whereas AICAr reduced the incorporation of palmitate into rough microsomes by ~50%. Palmitate incorporation into mitochondria was also reduced in the presence of AICAr by ~30%. The latter likely reflects a combination of decreased palmitate incorporation into rough microsomal membranes (which contaminate the crude mitochondrial fraction) and increased mitochondrial oxidation of palmitate.

The distribution of palmitate observed with a nontoxic concentration of palmitate (5 μM) was nearly identical to that observed with 500 μM (Fig. 1B), suggesting that the initial trafficking of this fatty acid to various subcellular locations is not concentration-dependent. In contrast, the relative distribution of 2-bromopalmitate, used as a nonlipotoxic control, was markedly different, with the bulk of the label remaining in the cytosol (Fig. 1B). This modified fatty acid is not as good a substrate for acyl-CoA synthetases (37), resulting in limited uptake and toxicity compared with palmitate (4.4 ± 0.8% and 5.2 ± 0.4% cell death at 24 h for control and 500 μM 2-bromopalmitate, respectively).

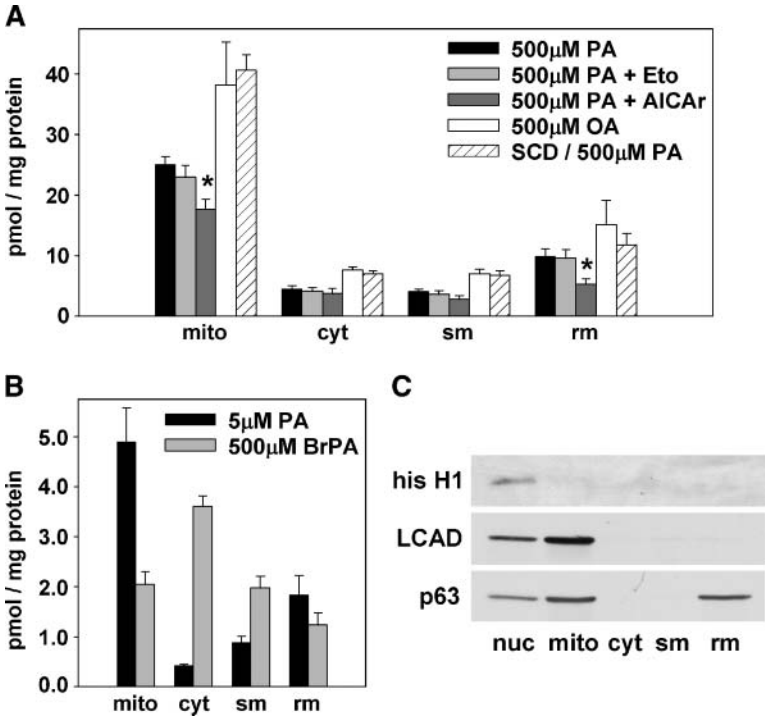

Fig. 1. Subcellular distribution of tritiated palmitate, oleate, and 2-bromopalmitate in wild-type and stearoyl-coenzyme A desaturase 1 (SCD1)-overexpressing CHO cells. A, B: Wild-type CHO (solid bars) or SCD1-overexpressing CHO (cross-hatched bars) cells were incubated for 1 h with 10 μCi/mmol [9,10-^{3}H]palmitate, [9,10-^{3}H]oleate, or [9,10-^{3}H]2-bromopalmitate, at the indicated concentrations of palmitate (PA), oleate (OA), or 2-bromopalmitate (BrPA). Graphs show radiolabel distribution in fractions isolated by sequential centrifugation. For experiments including etomoxir (Eto; 200 μM) or 5-aminoimidazole-4-carboxamide-1-β-4-ribofuranoside (AICAr; 500 μM), cells were incubated for 30 min with either compound before the addition of radiolabel and both etomoxir and AICAr were included for the subsequent incubation. Values are means ± SEM (n = 4). * $P < 0.05$. C: Immunoblotting of subcellular fractions for marker proteins. Histone H1 (his H1) was used as a marker for crude nuclei (nuc), long-chain acyl-CoA dehydrogenase (LCAD) was used for crude mitochondria (mito), and p63 was used for rough endoplasmic reticulum (ER) membranes (rm). cyt, cytosol; sm, smooth microsomes.

TABLE 1. Distribution of deuterated palmitate in rough microsomes from CHO cells

Lipid Species	Total Lipid	Deuterated Lipid	Distribution of Label	Deuterated Lipid/Total Lipid
	nmol/mg protein		%	
PC	58.01 ± 6.49	4.15 ± 0.65	42.09 ± 5.47	7.12 ± 0.48
PA	2.02 ± 0.21	0.00 ± 0.00	0.00 ± 0.00	0.00 ± 0.00
PG	2.83 ± 0.33	0.00 ± 0.00	0.00 ± 0.00	0.00 ± 0.00
PI	6.97 ± 0.24	0.22 ± 0.03	2.26 ± 0.27	3.19 ± 0.38
LPC	1.39 ± 0.25	0.21 ± 0.02	2.13 ± 0.09	15.71 ± 1.61
SM	7.09 ± 1.37	0.12 ± 0.06	1.16 ± 0.58	1.46 ± 0.50
Cer	0.34 ± 0.06	0.06 ± 0.01	0.65 ± 0.08	19.06 ± 1.04
FFA	31.06 ± 0.24	2.93 ± 0.52	30.42 ± 6.62	9.42 ± 1.61
TAG	5.60 ± 1.05	2.12 ± 0.60	21.29 ± 5.67	36.37 ± 4.13
Total	115.29 ± 8.29	9.82 ± 0.42	100	8.59 ± 0.61

CHO cells were incubated for 1 h with 500 μM [7,7,8,8-^{2}H]palmitate complexed to BSA at a molar ratio of 2:1. Rough microsomes were isolated by sequential centrifugation. Lipids were extracted and quantitated by electrospray ionization mass spectrometry. PC, phosphatidylcholine; PA, phosphatidic acid; PG, phosphatidylglycerol; PI, phosphatidylinositol; LPC, lysophosphatidylcholine; SM, sphingomyelin; Cer, ceramide; TAG, triacylglycerol. Values are means ± SEM.

To assess the consequences of palmitate incorporation into rough microsomes on the composition of these membranes, we analyzed both newly synthesized and total lipids in this fraction after a 1 h incubation with 500 μM [^{2}H]palmitate. The largest percentage of exogenous palmitate was incorporated into phosphatidylcholine (PC) species. However, significant proportions also remained as FFA or were incorporated into TAG species (**Table 1**, column 4). Overall, rough microsomes were composed primarily of PC and FFA, with very limited TAG content, corresponding to 50, 27, and 5% of the examined lipid mass content, respectively (Table 1, column 2). Thus, the labeled proportions of the rough microsomal pools of PC and FFA were relatively small, whereas the labeled proportion of the rough microsomal pool of TAG was significantly larger (Table 1, column 5). Unsaturated FAs make up the vast majority (81%) of acyl chain substituents in CHO cells under basal conditions (**Table 2**). Strikingly, the proportions of saturated PC and TAG in these membranes were increased by 1.5-fold (from 1.56% to 2.40%) and 3.0-fold (from 6.39% to 19.59%), respectively, with no significant change in total content of lipid species (Table 2). Thus, the remodeling of PC and TAG species accounted for a significant 1.3-fold increase (from 18.55% to 24.91%) in the saturated lipid content of rough microsomes from CHO cells incubated for 1 h with 500 μM palmitate.

Palmitate induces dramatic changes in ER structure and integrity

Increased saturation of lipid species is associated with a stiffening of cellular membranes (24–26). Based on our observations of increased saturation of PC and TAG species in rough microsomes from palmitate-treated CHO cells, we studied the effect of this treatment on the morphology of the ER. In electron micrographs of untreated cells, the ER appeared as normal, tubular cisternae delimited by electron-dense dots corresponding to ribosomes (**Fig. 2A**). In contrast, cells treated for 5 h with 500 μM palmitate contained numerous distended structures delimited by electron-dense ribosomes (Fig. 2B–D), a morphology consistent with the presence of markedly dilated rough ER (38). To determine whether this dramatic change in ER structure could be the result of palmitate-induced ROS generation, we compared the morphology of palmitate-treated cells with that of cells treated for 5 h with 2.5 mM H_2O_2. These conditions induced approximately the same

TABLE 2. Lipid composition of rough microsomes from CHO cells

	Control			Palmitate-Treated		
Lipid Species	Total Lipid (TL)	Saturated Lipid (SL)	SL/TL	Total Lipid (TL)	Saturated Lipid (SL)	SL/TL
	nmol/mg protein		%	*nmol/mg protein*		%
PC	80.69 ± 11.73	1.22 ± 0.10	1.56 ± 0.15	58.01 ± 6.49	1.43 ± 0.31	2.40 ± 0.27[a]
PA	2.27 ± 0.12	0.00 ± 0.00	0.00 ± 0.00	2.02 ± 0.21	0.00 ± 0.00	0.00 ± 0.00
PG	3.63 ± 0.26	0.29 ± 0.02	7.90 ± 0.19	2.83 ± 0.33	0.23 ± 0.05	8.06 ± 0.87
PI	10.79 ± 1.55	0.00 ± 0.00	0.00 ± 0.00	6.97 ± 0.24	0.00 ± 0.00	0.00 ± 0.00
LPC	2.48 ± 0.53	1.46 ± 0.35	58.07 ± 1.90	1.39 ± 0.25	0.83 ± 0.13	60.70 ± 2.41
SM	8.28 ± 1.28	5.84 ± 1.09	69.63 ± 3.24	7.09 ± 1.37	4.98 ± 0.88	70.72 ± 1.52
Cer	0.66 ± 0.12	0.49 ± 0.10	73.56 ± 3.70	0.34 ± 0.06	0.24 ± 0.05	68.68 ± 2.86
FFA	29.29 ± 1.02	16.91 ± 0.94	57.65 ± 1.51	31.06 ± 0.24	19.69 ± 0.29[a]	63.40 ± 0.81
TAG	5.96 ± 0.13	0.38 ± 0.00	6.39 ± 0.14	5.60 ± 1.05	1.16 ± 0.37	19.59 ± 3.09[a]
Total	144.04 ± 16.41	26.58 ± 2.51	18.55 ± 0.46	115.29 ± 8.29	28.56 ± 1.08	24.91 ± 1.10[a]

CHO cells were incubated for 1 h with 500 μM [7,7,8,8-^{2}H]palmitate complexed to BSA at a molar ratio of 2:1. Rough microsomes were isolated by sequential centrifugation. Lipids were extracted and quantitated by electrospray ionization mass spectrometry. Values are means ± SEM.
[a] $P < 0.05$ for control versus palmitate-treated.

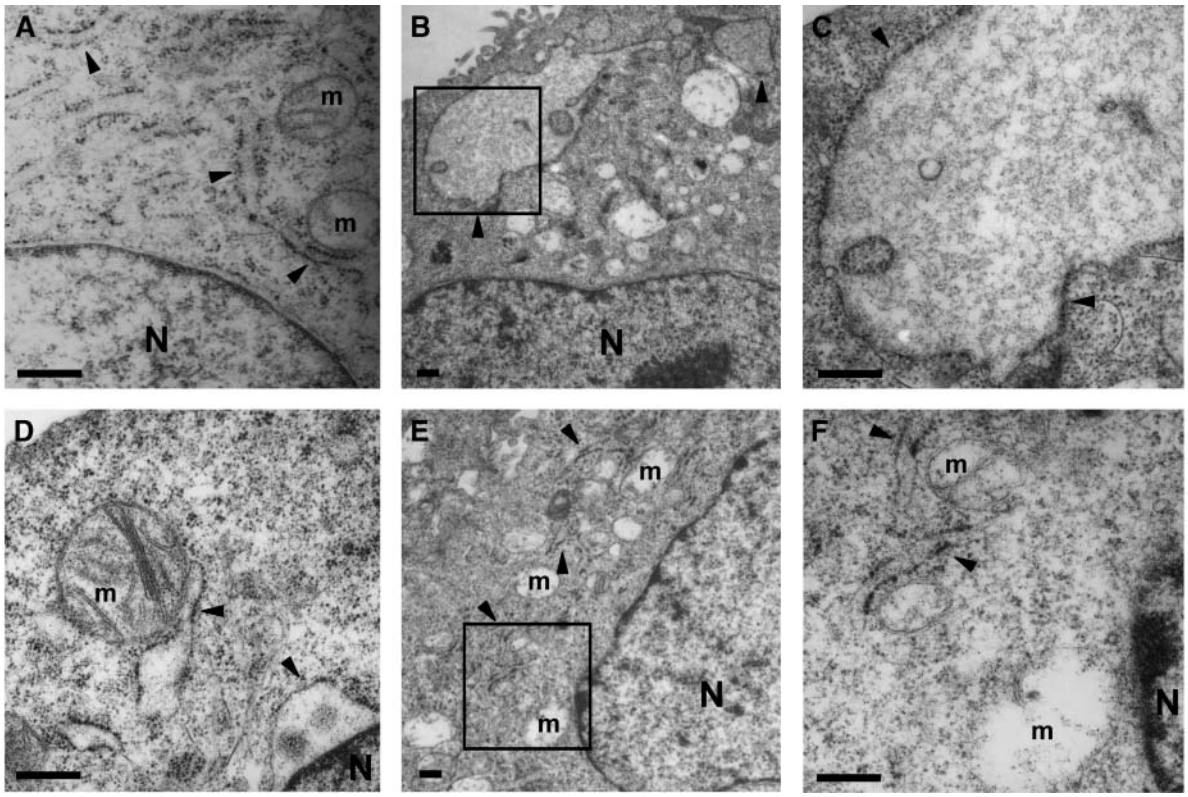

Fig. 2. Incubation of CHO cells with palmitate, but not H_2O_2, results in dilatation of the ER. CHO cells were incubated for 5 h in the absence (A) or presence of either 500 μM palmitate (B–D) or 2.5 mM H_2O_2 (E, F). Morphological changes were observed by transmission electron microscopy. C and F show enlarged views of boxed areas in B and E, respectively. Arrowheads indicate rough ER cisternae delimited by electron-dense ribosomes. m, mitochondria; N, nuclei. Bars = 275 nm.

amount of cell death within 24 h (16.8 ± 2.9% and 21.1 ± 1.5% cell death for 500 μM palmitate and 2.5 mM H_2O_2, respectively). In contrast to cells treated with palmitate, those treated with H_2O_2 contained normal ER cisternae (Fig. 2E). However, the mitochondria in H_2O_2-treated cells appeared compromised compared with both control and palmitate-treated cells (Fig. 2F vs. 2A, D).

We next assessed whether the changes in ER structure observed in response to palmitate were associated with evidence of compromised ER integrity, and further, whether any changes in ER integrity were dependent on the induction of oxidative stress. Isolation and immunoblotting of cytosol and crude membrane/organelle fractions from CHO cells incubated for 5 h with 500 μM palmitate resulted in the escape of protein-folding chaperones, GRP78 (78 kDa) (**Fig. 3A**) and PDI (58 kDa) (Fig. 3B), from the ER to the cytosol. These observations are broadly consistent with those recently observed in palmitate-treated pancreatic β-cells (39). Levels of the integral ER membrane protein, p63, were unaltered and indicate the relative purity of our cytosolic and membrane fractions. Although α-tocopherol (vitamin E) prevents palmitate-induced ROS accumulation within 5 h (14), incubation with palmitate in the presence of 200 μM vitamin E did not prevent the redistribution of normally ER lumenal proteins. Furthermore, these effects were not observed in cells incubated for 5 h with 2.5 mM H_2O_2. Conditions that result in the incorporation of unsaturated FA into ER membranes, including incubation of wild-type CHO cells with 500 μM oleate and SCD1-overexpressing cells with 500 μM palmitate, did not alter the distribution of ER chaperone proteins (Fig. 3). Together with our observations of dramatically altered ER morphology (Fig. 2), these data suggest that the detrimental effects of palmitate on ER structure and integrity are distinct from changes induced by severe oxidative stress.

Palmitate induces changes in mitochondrial function

Both palmitate-induced alterations of ER structure and integrity and palmitate-induced oxidative stress could initiate the flux of calcium from the ER to the mitochondria and lead to the loss of mitochondrial membrane potential. Thus, we determined whether incubation with palmitate resulted in the rapid depletion of ER calcium. Assays of thapsigargin-sensitive calcium revealed that ER stores were significantly reduced after 15 min and by up to 25% after 30 min with 500 μM palmitate, but not with the nontoxic, unsaturated fatty acid, oleate (**Fig. 4A**). This depletion of ER calcium was followed by the gradual escape of protein-folding chaperones, GRP78 (Fig. 4B) and PDI (Fig. 4C), from the ER to the cytosol over the course of 5 h.

Previous studies have demonstrated an impairment of mitochondrial function late in the response to lipotoxic

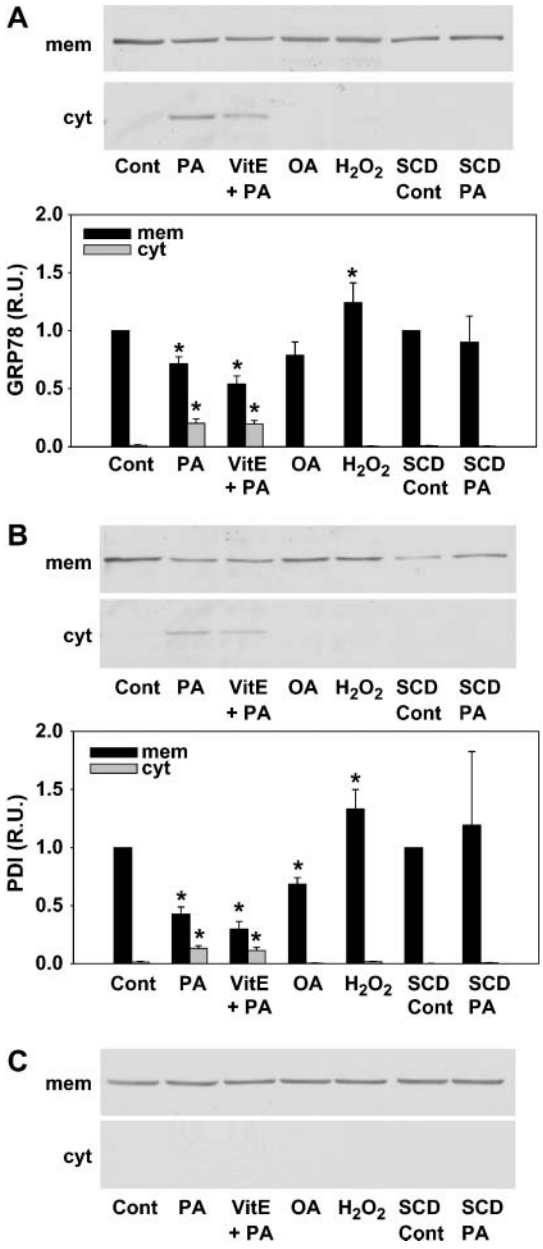

Fig. 3. Incubation of CHO cells with palmitate results in the escape of protein-folding chaperones from the ER to the cytosol. Membrane/organelle (mem) and cytosolic (cyt) fractions were isolated by sequential detergent extraction from wild-type CHO and SCD1-overexpressing CHO (SCD) cells incubated for 5 h in the absence (Cont) or presence of 500 μM palmitate (PA), 500 μM oleate (OA), or 2.5 mM H_2O_2. For conditions including α-tocopherol (VitE; 200 μM), cells were incubated for 30 min with the antioxidant before the addition of palmitate, and α-tocopherol was included for the subsequent incubation. Relative glucose-regulated protein 78 (GRP78; A), protein disulfide isomerase (PDI; B), and p63 (C) protein levels in each fraction were detected by immunoblotting. Blots representative of four independent experiments are shown, with densitometric analyses displayed immediately below in relative units (R.U.). Values are means ± SEM (n = 4). * $P < 0.05$ compared with control fractions.

stress (9). Thus, we determined whether the rapid depletion of ER calcium in response to palmitate is accompanied by changes in mitochondrial function. Isolation and immunoblotting of crude mitochondrial and cytosolic fractions revealed that 30 min of incubation with 500 μM palmitate reduced mitochondrial cytochrome c (15 kDa) content by 40% (Fig. 4D). However, no change in cytochrome c content was detected after 15 min with palmitate, and the protein was not detected in the cytosol over the entire course of palmitate treatment (Fig. 4D). Mitochondrial long-chain acyl-CoA dehydrogenase content was not affected by palmitate (data not shown). Assessment of mitochondrial membrane potential, by JC-1 staining and flow cytometry, revealed significant reductions in the ratios of red (FL2) to green (FL1) fluorescence, indicative of mitochondrial depolarization, only after extended (5 h) incubations with either 500 μM palmitate or 2.5 mM H_2O_2 (Fig. 4E). The relative abundance of intact mitochondria, assessed by staining with MitoTracker Green FM and flow cytometry, was not significantly reduced after 5 h with 500 μM palmitate, as shown by the lack of change in mean fluorescence (Fig. 4F). However, consistent with our morphological analyses (Fig. 2), incubation for 5 h with 2.5 mM H_2O_2 reduced mean fluorescence by 37%. Incubation for 18 h with 500 μM palmitate reduced mean fluorescence by 46%. Together, these data suggest that palmitate-induced changes in ER calcium content may precede the gross impairment of mitochondrial function.

Palmitate-induced changes in ER integrity are reduced by increasing β-oxidation

Based on our observations of the subcellular distribution of [^{3}H]palmitate in the presence of AICAr (Fig. 1A), we hypothesized that channeling palmitate toward β-oxidation would prevent the detrimental changes in ER integrity associated with its incorporation into ER membrane PC and TAG (Tables 1, 2). Consistent with this hypothesis, AICAr decreased the palmitate-induced escape of GRP78 (**Fig. 5A**) and PDI (Fig. 5B) from the ER to the cytosol by 42% and 50%, respectively (Fig. 5C), and reduced eventual cell death by 30% (Fig. 5C). Conversely, incubation with etomoxir, at a concentration that inhibits β-oxidation, decreased neither chaperone escape nor cell death. In fact, etomoxir treatment tended to increase cell death at 48 h. Thus, increasing β-oxidation diminishes palmitate-induced changes in ER integrity and cell death.

Palmitate-induced changes in ER integrity, followed by caspase activation and cell death, occur in cardiomyoblasts

To extend these findings to a cell type more relevant to lipotoxic disease, we determined the distribution of ER protein-folding chaperones in response to palmitate in H9c2 rat cardiomyoblasts. In experiments similar to those performed in CHO cells, H9c2 cells were incubated for up to 5 h with 500 μM palmitate. Subsequent isolation and immunoblotting of cytosol and crude membrane/organelle fractions revealed that, as was observed in CHO cells,

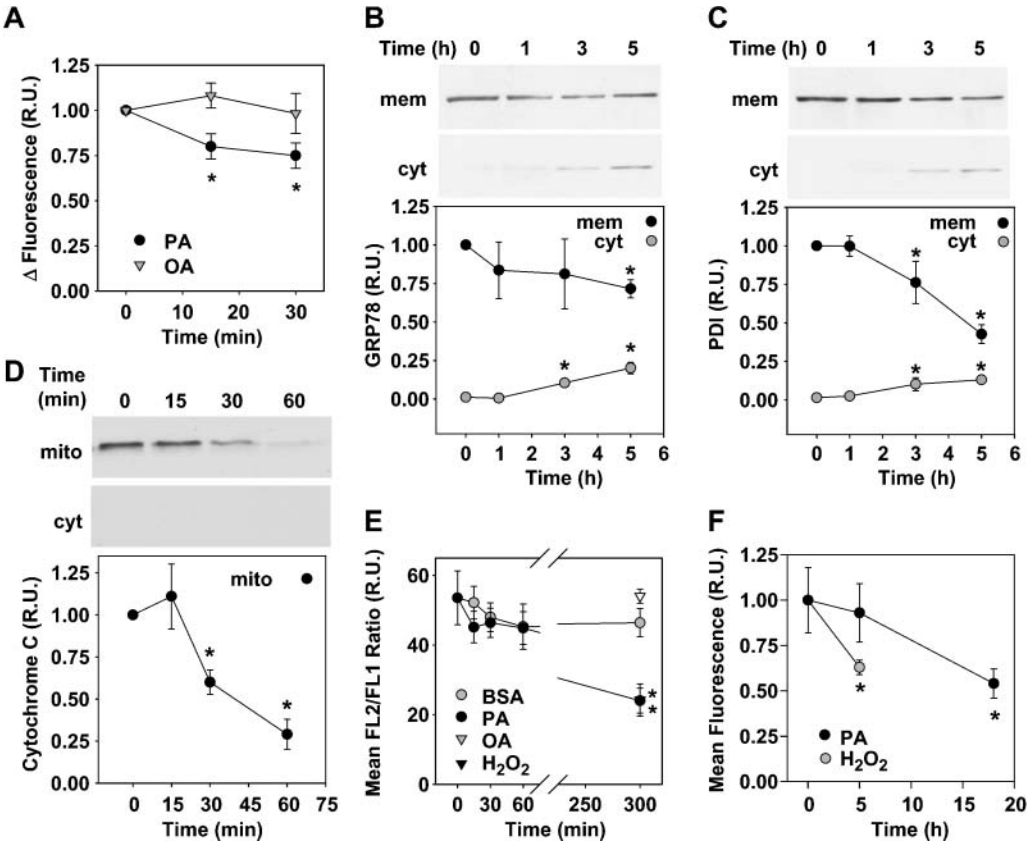

Fig. 4. Palmitate-induced changes in ER calcium and chaperone content occur early and may precede gross impairment of mitochondrial function. Wild-type CHO cells were incubated for the indicated times with 500 μM palmitate (PA), 500 μM oleate (OA), or 2.5 mM H_2O_2. A: Palmitate-induced depletion of thapsigargin-sensitive ER calcium stores was assessed using Fluo-4 AM. Values represent relative increment in fluorescence (Δ fluorescence) upon addition of thapsigargin (1 μM; n = 4). B, C: Membrane/organelle (mem) and cytosolic (cyt) fractions were isolated by sequential detergent extraction from CHO cells incubated for up to 5 h with 500 μM palmitate. Relative GRP78 (B) and PDI (C) protein levels in each fraction were detected by immunoblotting. Blots representative of four independent experiments are shown, with densitometric analyses displayed immediately below in relative units (R.U.). D: Crude mitochondrial (mito) and cytosolic (cyt) fractions were isolated by sequential centrifugation from CHO cells incubated for up to 60 min with 500 μM palmitate. Relative cytochrome c protein levels in each fraction were detected by immunoblotting and analyzed as described for B and C. E: Mitochondrial depolarization was assessed in CHO cells incubated for up to 5 h with BSA (control), 500 μM palmitate, 500 μM oleate, or 2.5 mM H_2O_2 by staining with JC-1. Mean red and green fluorescence were determined by flow cytometry for subsequent calculation of FL2/FL1 ratios (n = 5). F: The presence of intact mitochondria was assessed in CHO cells incubated for up to 18 h with either 500 μM palmitate or 2.5 mM H_2O_2 by staining with MitoTracker Green FM. Mean fluorescence was determined by flow cytometry (n = 3). All values are means ± SEM. * $P < 0.05$ compared with 0 h.

incubation with palmitate resulted in the appearance of GRP78 (**Fig. 6A**) and PDI (Fig. 6B) in the cytosol.

Although palmitate-induced cell death is characterized by markers of apoptosis, including cytochrome c release, caspase-3 activation, and DNA fragmentation, we previously observed that caspase-3 activation in response to palmitate is relatively modest compared with other inducers of apoptosis (14), raising the possibility that other caspases may play an important role. Based on the dramatic effects observed on ER structure and integrity, we determined whether caspase-7, which is activated in response to ER stress and is the only effector caspase known to localize to the ER upon activation (40, 41), could also be activated in response to palmitate. H9c2 cells were incubated for up to 18 h with 500 μM palmitate. Subsequent subcellular fractionation and immunoblotting revealed that, in accordance with previous studies (13), cleaved (active) caspase-3 began to accumulate in the cytosol within 9 h of palmitate treatment (**Fig. 7A**). Within the same time frame, cleaved caspase-7 accumulated in the microsomal fraction of palmitate-treated cells, with a corresponding loss of pro-caspase-7 from the cytosol (Fig. 7B). Furthermore, increasing β-oxidation with the AMPK activator, AICAr, decreased palmitate-induced activation of caspase-3 and -7 by 46% and 49%, respectively (Fig. 7C), and reduced eventual cell death by 23% (Fig. 7D). In contrast, inhibition of β-oxidation with etomoxir increased caspase activation and, as was observed in CHO

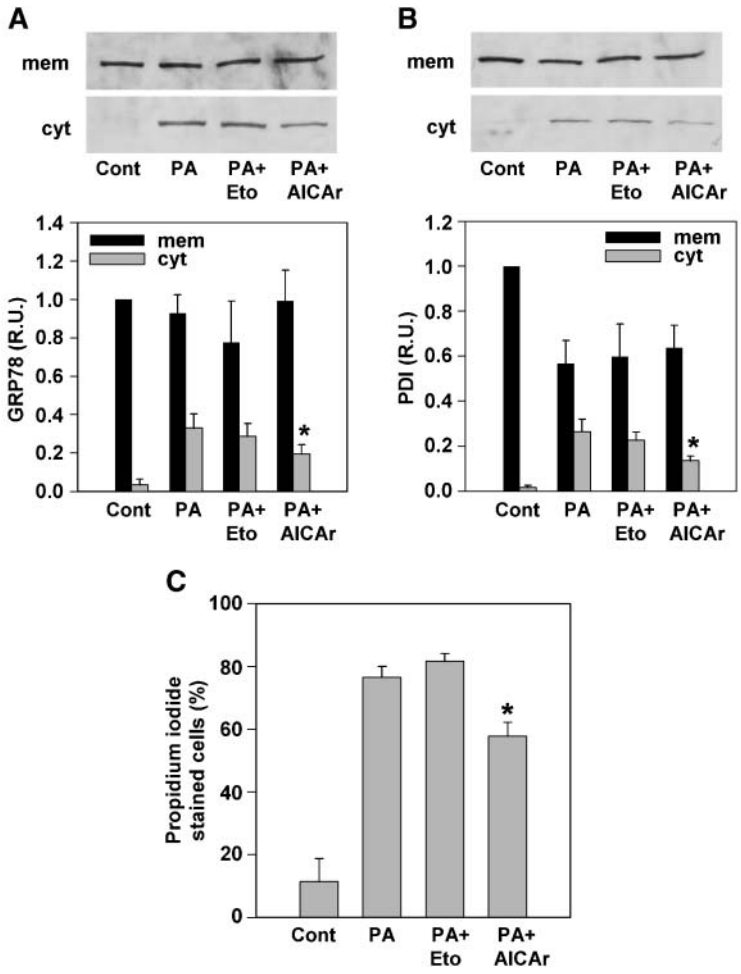

Fig. 5. Palmitate-induced changes in ER integrity and subsequent cell death are reduced by increasing β-oxidation. A, B: Membrane/organelle (mem) and cytosolic (cyt) fractions were isolated by sequential detergent extraction from CHO cells incubated for 5 h with 500 μM palmitate (PA). For conditions including etomoxir (Eto; 200 μM) or AICAr (500 μM), cells were incubated for 30 min with either compound before the addition of palmitate, and both etomoxir and AICAr were included for the subsequent incubation. Relative GRP78 (A) and PDI (B) protein levels in each fraction were detected by immunoblotting. Blots representative of four independent experiments are shown, with densitometric analyses displayed immediately below in relative units (R.U.). C: CHO cells were incubated with 500 μM palmitate plus etomoxir or AICAr as described for A and B. Cell death was determined after 48 h by propidium iodide staining and flow cytometry (n = 3). All values are means ± SEM. * $P < 0.05$ compared with control (Cont).

cells, trended toward increased cell death. Together, these data indicate that palmitate-induced changes in ER integrity precede caspase-3 and -7 activation and cell death in cardiomyoblasts. Furthermore, increasing β-oxidation diminishes palmitate-induced caspase activation and cell death.

DISCUSSION

ER stress was recently linked to the pathogenesis of several diseases, including insulin resistance and type 2 diabetes (reviewed in Refs. 42, 43). Although glucose toxicity has been implicated in the induction of ER stress in

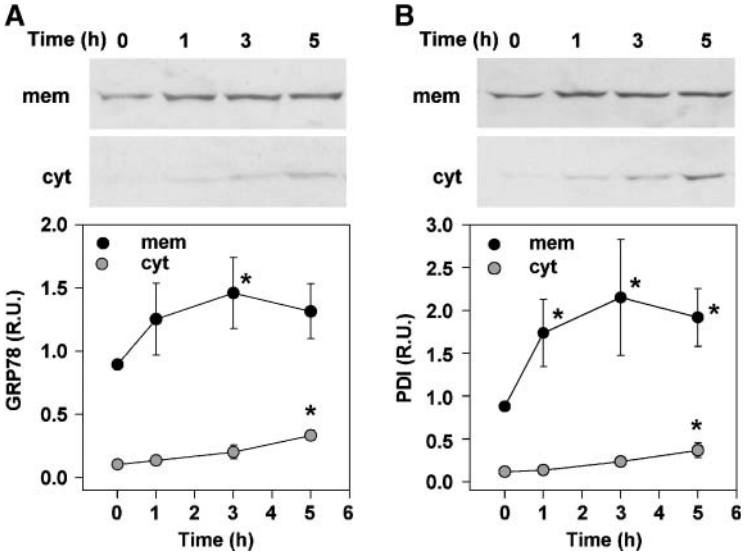

Fig. 6. Incubation of cardiomyoblasts with a lipotoxic concentration of palmitate results in the escape of protein-folding chaperones from the ER to the cytosol. Microsomal (mem) and cytosolic (cyt) fractions were isolated by sequential centrifugation from H9c2 myoblasts incubated for up to 5 h with growth medium supplemented with 500 μM palmitate. Relative GRP78 (A) and PDI (B) protein levels in each fraction were detected by immunoblotting. Blots shown are representative of four independent experiments, with densitometric analyses displayed immediately below in relative units (R.U.). Values are means ± SEM. * $P < 0.05$ compared with 0 h.

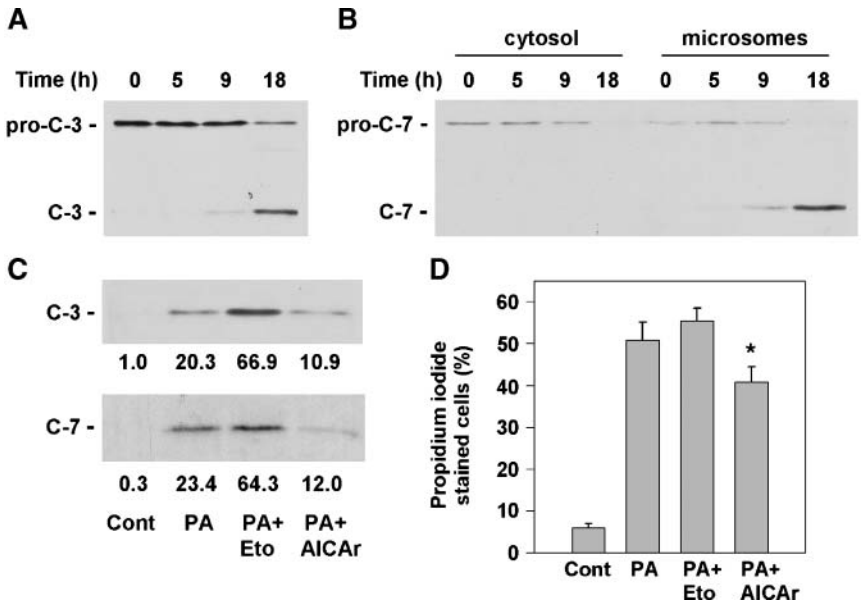

Fig. 7. Palmitate-induced activation of caspase-3 and -7, and subsequent cell death, are reduced by increasing β-oxidation in H9c2 cardiomyoblasts. A, B: Cytosolic and microsomal fractions were isolated by sequential centrifugation from undifferentiated H9c2 cells incubated for up to 18 h with 500 μM palmitate. Pro-caspase-3 (pro-C-3) and active caspase-3 (C-3) (A) were detected by immunoblotting cytosolic fractions. Pro-caspase-7 (pro-C-7) and active caspase-7 (C-7) (B) were detected by immunoblotting cytosolic and microsomal fractions, respectively. C: Active caspase-3 and -7 were detected in whole cell lysates from cells incubated for 14 h with 500 μM palmitate (PA). For conditions including etomoxir (Eto; 200 μM) or AICAr (500 μM), cells were incubated for 30 min with either compound before the addition of palmitate, and both etomoxir and AICAr were included for the subsequent incubation. Mean relative densitometric values, in relative units (R.U.), for four independent experiments are given below each band. D: Cells were incubated with 500 μM palmitate plus etomoxir or AICAr as described for C. Cell death was determined after 24 h by propidium iodide staining and flow cytometry (n = 4). All values are means ± SEM. * $P < 0.05$ compared with palmitate-treated cells. Cont, control.

type 2 diabetes (reviewed in Ref. 44), this disease is characterized by pleiotropic metabolic abnormalities, including increased serum TAG and FA levels, that may also be detrimental. In fact, recent studies in cultured pancreatic β-cells (19), hepatocytes (20), and cardiomyoblasts (14) indicate that FA overload also induces ER stress, leading to apoptotic cell death. Furthermore, our studies in cardiomyoblasts suggested that the mechanism whereby palmitate overload rapidly induced ER stress involved the generation of ROS (14). In addition, our observations in MHC-ACS mice, a model of cardiac-specific lipotoxicity, revealed that increased FA uptake in vivo is associated with oxidative and ER stress and cardiomyocyte death (5, 14).

In this study, we show that palmitate overload rapidly increases the saturation of PC and TAG in ER membranes, which is associated with the subsequent compromise of ER structure and integrity. The effect on ER integrity observed in wild-type CHO cells treated with palmitate is not observed in CHO cells treated with oleate or in SCD1-overexpressing CHO cells treated with palmitate. In all three conditions, the relative distributions of exogenous FA between the ER and mitochondria are comparable, but in the latter two conditions, exogenous FAs are either unsaturated or can be efficiently desaturated at the ER. We have shown previously that the remodeling of TAG species observed in SCD1-overexpressing CHO cells treated with palmitate is not as extensive as that observed in wild-type CHO cells treated with palmitate (27). The effects of palmitate on ER structure and integrity were distinct from the changes induced by severe oxidative stress, and the effects of palmitate on ER integrity were not prevented by vitamin E. In light of our previous (14) and current observations, we suggest that the deleterious effect of palmitate on the ER is twofold: *i*) palmitate induces the generation of ROS, leading to ER stress, activation of the unfolded protein response, and subsequent induction of apoptosis (14); and *ii*) palmitate alters ER membrane composition, leading to dramatic changes in ER structure and integrity. The latter may also contribute to the initiation of ER stress. Consistent with this concept, recent studies in rodent models of hepatic steatosis, characterized by an increase in saturated microsomal membrane phospholipid content, demonstrated hepatocyte ER stress preceding apoptosis (45). Thus, impairment of the structure and function of this organelle appears to play an early and important role in the cellular response to fatty acid overload.

Palmitate-induced cell death is characterized by markers of mitochondria-mediated apoptosis, including the loss of mitochondrial membrane potential, mitochondrial swelling, and cytochrome c release into the cytosol (reviewed in Ref. 8). Previous studies suggest that these events occur relatively late in the process of lipotoxic cell death (9) and

may be initiated by decreased cardiolipin synthesis (11), increased ceramide synthesis (9, 46), JNK activation (47), and increased ROS generation (13), which have been documented at >5 h after incubation with palmitate. The depletion of thapsigargin-sensitive ER calcium stores we observed after 15 min of palmitate overload is consistent with both the onset of oxidative stress (14) and the remodeling of ER membrane lipids leading to impaired organelle structure and integrity. Similar depletion of calcium stores, attributed to the disrupted function of sarcoplasmic ER calcium ATPase, has been observed during macrophage foam cell formation, a condition that results in reduced fluidity of ER membranes as a result of enrichment with free cholesterol (48, 49). It is established that calcium flux from the ER to the mitochondria can trigger mitochondrial permeability transition and initiate mitochondrial pathways of apoptosis (15, 16, 50). Because the palmitate-induced changes we observed in ER calcium content preceded the impairment of mitochondrial function, as assessed by measurements of cytochrome c depletion and membrane depolarization, our studies suggest that the ER may play a proximal role in lipotoxic cell death. However, it is not possible to exclude concomitant direct effects of palmitate on the mitochondria.

Our study also suggests that the channeling of excess FA toward β-oxidation and oxidative phosphorylation is not detrimental. First, similar relative distributions of FA to the mitochondria are observed in oleate-supplemented wild-type CHO cells, palmitate-supplemented SCD1-overexpressing CHO cells, and palmitate-supplemented wild-type CHO cells. Yet, only the latter condition is associated with lipotoxic cell death. Second, consistent with previous studies (35, 36, 47), we show that increasing β-oxidation, through stimulation of AMPK with AICAr, diminishes lipotoxic cell death. We extend these observations by showing that AICAr reduces the incorporation of palmitate into ER membranes, thereby preserving ER integrity. And third, decreasing β-oxidation, through inhibition of carnitine palmitoyl transferase 1 with etomoxir, leads to further increases in caspase activation and trends toward increased cell death, rather than decreased lipotoxicity.

Although palmitate-induced cell death is characterized by markers of apoptosis, including cytochrome c release, caspase-3 activation, and DNA fragmentation, we previously observed that caspase-3 activation in response to palmitate is relatively modest compared with other inducers of apoptosis (14). Here, we demonstrate that the effector caspase-7 is activated in response to palmitate overload within the same time frame as caspase-3. This caspase has been implicated previously in palmitate-induced apoptosis in a caspase-3-deficient breast cancer cell line (51). Because caspase-7 is activated in response to ER stress and is the only effector caspase known to localize to the ER upon activation (40, 41), its activation upon incubation with palmitate further supports an important role for the ER in the lipotoxic response.

The composition of lipid membranes has dramatic effects on membrane properties (52). Although the stability of all membrane proteins is sensitive to membrane composition, the activity of transport proteins is particularly sensitive (49, 53, 54). In addition, the acyl chains of lipids directly affect the fusion/fission events of membranes (22, 23). Therefore, it is likely that the changes in ER lipid composition we have observed in response to palmitate overload broadly influence ER membrane functions, including transport and membrane dynamics. Based on our current and previous (14) studies, we suggest the following model for the role of the ER in palmitate-induced cell death. Saturated FA overload in nonadipose tissues overwhelms the cellular capacity to store FAs as triglycerides or to use them for energy. This FA overload can lead to the production of ROS from several potential sources, which in turn can induce ER stress (14). As demonstrated here, palmitate can also be incorporated rapidly into complex lipids in the ER membrane. Increased saturation of ER membrane PC and TAG may result in dramatic impairment of the structure and integrity of the organelle and may contribute to ER stress. Both oxidative stress and altered ER composition and integrity could result in the release of ER calcium stores, triggering apoptotic cell death via the mitochondria (**Fig. 8**). Together with the observation that ER stress is central to cholesterol-induced apoptosis in macrophages (48, 49, 55), our results may be consistent with a more general paradigm in which perturbations of cellular lipid metabolism can result in a death response initiated by events occurring at the ER. These studies suggest that ER may be a proximal target for therapies aimed at improving cellular function in the setting of lipid metabolic disorders.

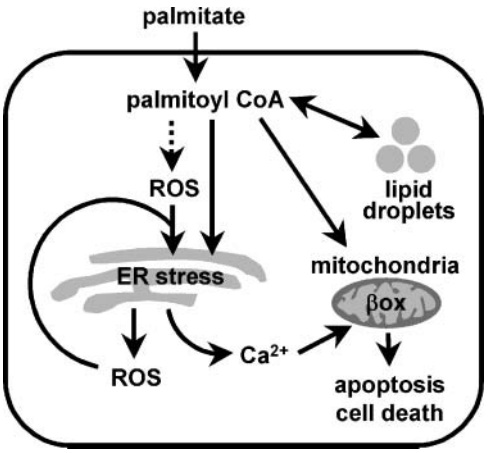

Fig. 8. Model for the role of the ER in palmitate-induced cell death. Under conditions of saturated FA overload in nonadipose tissues, the cellular capacity to store these FAs as triglycerides or to oxidize them for energy (βox) is overwhelmed. This FA overload can lead to the production of reactive oxygen species (ROS), from several potential sources, which can in turn induce ER stress. Palmitate can also be rapidly incorporated into complex lipids in the ER membrane. Increased saturation of ER membrane lipids is associated with dramatic impairment of the structure and integrity of the organelle. Both oxidative stress and altered ER composition and integrity could result in the release of ER calcium (Ca^{2+}) stores, triggering apoptotic cell death via the mitochondria.

The authors thank Marilyn Levy of the Morphology Core at the Washington University School of Medicine for the expert

preparation of thin sections and electron micrographs and Dr. Paul Schlesinger from the Department of Physiology and Cell Biology at the Washington University School of Medicine for critical reading of the manuscript. This work was supported by grants from the National Institutes of Health (DK-064989 to J.E.S.; HL-57278 to X.H.). N.M.B. is supported by a Research Fellowship from the Heart and Stroke Foundation of Canada.

REFERENCES

1. Unger, R. H. 2003. Lipid overload and overflow: metabolic trauma and the metabolic syndrome. *Trends Endocrinol. Metab.* **14:** 398–403.
2. Zhou, Y. T., P. Grayburn, A. Karim, M. Shimabukuro, M. Higa, D. Baetens, L. Orci, and R. H. Unger. 2000. Lipotoxic heart disease in obese rats: implications for human obesity. *Proc. Natl. Acad. Sci. USA.* **97:** 1784–1789.
3. Aasum, E., D. D. Belke, D. L. Severson, R. A. Riemersma, M. Cooper, M. Andreassen, and T. S. Larsen. 2002. Cardiac function and metabolism in type 2 diabetic mice after treatment with BM 17.0744, a novel PPAR-alpha activator. *Am. J. Physiol. Heart Circ. Physiol.* **283:** H949–H957.
4. Christoffersen, C., E. Bollano, M. L. Lindegaard, E. D. Bartels, J. P. Goetze, C. B. Andersen, and L. B. Nielsen. 2003. Cardiac lipid accumulation associated with diastolic dysfunction in obese mice. *Endocrinology.* **144:** 3483–3490.
5. Chiu, H. C., A. Kovacs, D. A. Ford, F. F. Hsu, R. Garcia, P. Herrero, J. E. Saffitz, and J. E. Schaffer. 2001. A novel mouse model of lipotoxic cardiomyopathy. *J. Clin. Invest.* **107:** 813–822.
6. Yagyu, H., G. Chen, M. Yokoyama, K. Hirata, A. Augustus, Y. Kako, T. Seo, Y. Hu, E. P. Lutz, M. Merkel, et al. 2003. Lipoprotein lipase (LpL) on the surface of cardiomyocytes increases lipid uptake and produces a cardiomyopathy. *J. Clin. Invest.* **111:** 419–426.
7. Chiu, H. C., A. Kovacs, R. M. Blanton, X. Han, M. Courtois, C. J. Weinheimer, K. A. Yamada, S. Brunet, H. Xu, J. M. Nerbonne, et al. 2005. Transgenic expression of fatty acid transport protein 1 in the heart causes lipotoxic cardiomyopathy. *Circ. Res.* **96:** 225–233.
8. Borradaile, N. M., and J. E. Schaffer. 2005. Lipotoxicity in the heart. *Curr. Hypertens. Rep.* **7:** 412–417.
9. Sparagna, G. C., D. L. Hickson-Bick, L. M. Buja, and J. B. McMillin. 2000. A metabolic role for mitochondria in palmitate-induced cardiac myocyte apoptosis. *Am. J. Physiol. Heart Circ. Physiol.* **279:** H2124–H2132.
10. Kong, J. Y., and S. W. Rabkin. 2000. Palmitate-induced apoptosis in cardiomyocytes is mediated through alterations in mitochondria: prevention by cyclosporin A. *Biochim. Biophys. Acta.* **1485:** 45–55.
11. Ostrander, D. B., G. C. Sparagna, A. A. Amoscato, J. B. McMillin, and W. Dowhan. 2001. Decreased cardiolipin synthesis corresponds with cytochrome c release in palmitate-induced cardiomyocyte apoptosis. *J. Biol. Chem.* **276:** 38061–38067.
12. Dyntar, D., M. Eppenberger-Eberhardt, K. Maedler, M. Pruschy, H. M. Eppenberger, G. A. Spinas, and M. Y. Donath. 2001. Glucose and palmitic acid induce degeneration of myofibrils and modulate apoptosis in rat adult cardiomyocytes. *Diabetes.* **50:** 2105–2113.
13. Listenberger, L. L., D. S. Ory, and J. E. Schaffer. 2001. Palmitate-induced apoptosis can occur through a ceramide-independent pathway. *J. Biol. Chem.* **276:** 14890–14895.
14. Borradaile, N. M., K. K. Buhman, L. L. Listenberger, C. J. Magee, E. T. Morimoto, D. S. Ory, and J. E. Schaffer. 2006. A critical role for eukaryotic elongation factor 1A-1 in lipotoxic cell death. *Mol. Biol. Cell.* **17:** 770–778.
15. Demaurex, N., and C. Distelhorst. 2003. Cell biology. Apoptosis—the calcium connection. *Science.* **300:** 65–67.
16. Scorrano, L., S. A. Oakes, J. T. Opferman, E. H. Cheng, M. D. Sorcinelli, T. Pozzan, and S. J. Korsmeyer. 2003. BAX and BAK regulation of endoplasmic reticulum Ca^{2+}: a control point for apoptosis. *Science.* **300:** 135–139.
17. Rao, R. V., H. M. Ellerby, and D. E. Bredesen. 2004. Coupling endoplasmic reticulum stress to the cell death program. *Cell Death Differ.* **11:** 372–380.
18. Rutkowski, D. T., and R. J. Kaufman. 2004. A trip to the ER: coping with stress. *Trends Cell Biol.* **14:** 20–28.
19. Kharroubi, I., L. Ladriere, A. K. Cardozo, Z. Dogusan, M. Cnop, and D. L. Eizirik. 2004. Free fatty acids and cytokines induce pancreatic beta-cell apoptosis by different mechanisms: role of nuclear factor-kappaB and endoplasmic reticulum stress. *Endocrinology.* **145:** 5087–5096.
20. Wei, Y., D. Wang, F. Topczewski, and M. J. Pagliassotti. 2006. Saturated fatty acids induce endoplasmic reticulum stress and apoptosis independently of ceramide in liver cells. *Am. J. Physiol. Endocrinol. Metab.* **291:** E275–E281.
21. Turner, M. D. 2004. Fatty acyl CoA-mediated inhibition of endoplasmic reticulum assembly. *Biochim. Biophys. Acta.* **1693:** 1–4.
22. Kozlovsky, Y., L. V. Chernomordik, and M. M. Kozlov. 2002. Lipid intermediates in membrane fusion: formation, structure, and decay of hemifusion diaphragm. *Biophys. J.* **83:** 2634–2651.
23. Haque, M. E., and B. R. Lentz. 2004. Roles of curvature and hydrophobic interstice energy in fusion: studies of lipid perturbant effects. *Biochemistry.* **43:** 3507–3517.
24. Rintoul, D. A., L. A. Sklar, and R. D. Simoni. 1978. Membrane lipid modification of Chinese hamster ovary cells. Thermal properties of membrane phospholipids. *J. Biol. Chem.* **253:** 7447–7452.
25. Schroeder, F., and E. H. Goh. 1980. Effect of fatty acids on physical properties of microsomes from isolated perfused rat liver. *Chem. Phys. Lipids.* **26:** 207–224.
26. Spector, A. A., and M. A. Yorek. 1985. Membrane lipid composition and cellular function. *J. Lipid Res.* **26:** 1015–1035.
27. Listenberger, L. L., X. Han, S. E. Lewis, S. Cases, R. V. Farese, Jr., D. S. Ory, and J. E. Schaffer. 2003. Triglyceride accumulation protects against fatty acid-induced lipotoxicity. *Proc. Natl. Acad. Sci. USA.* **100:** 3077–3082.
28. Nigam, S. K., and G. Blobel. 1989. Cyclic AMP-dependent protein kinase in canine pancreatic rough endoplasmic reticulum. *J. Biol. Chem.* **264:** 16927–16932.
29. Hainline, B. E., D. J. Kahlenbeck, J. Grant, and A. W. Strauss. 1993. Tissue specific and developmental expression of rat long- and medium-chain acyl-CoA dehydrogenases. *Biochim. Biophys. Acta.* **1216:** 460–468.
30. Schweizer, A., J. Rohrer, J. W. Slot, H. J. Geuze, and S. Kornfeld. 1995. Reassessment of the subcellular localization of p63. *J. Cell Sci.* **108:** 2477–2485.
31. Han, X., and R. W. Gross. 2005. Shotgun lipidomics: multidimensional MS analysis of cellular lipidomes. *Expert Rev. Proteomics.* **2:** 253–264.
32. Han, X., and R. W. Gross. 2005. Shotgun lipidomics: electrospray ionization mass spectrometric analysis and quantitation of cellular lipidomes directly from crude extracts of biological samples. *Mass Spectrom. Rev.* **24:** 367–412.
33. Abdolzade-Bavil, A., S. Hayes, L. Goretzki, M. Kroger, J. Anders, and R. Hendriks. 2004. Convenient and versatile subcellular extraction procedure, that facilitates classical protein expression profiling and functional protein analysis. *Proteomics.* **4:** 1397–1405.
34. Nigam, S. K., A. L. Goldberg, S. Ho, M. F. Rohde, K. T. Bush, and M. Sherman. 1994. A set of endoplasmic reticulum proteins possessing properties of molecular chaperones includes Ca(2+)-binding proteins and members of the thioredoxin superfamily. *J. Biol. Chem.* **269:** 1744–1749.
35. El-Assaad, W., J. Buteau, M. L. Peyot, C. Nolan, R. Roduit, S. Hardy, E. Joly, G. Dbaibo, L. Rosenberg, and M. Prentki. 2003. Saturated fatty acids synergize with elevated glucose to cause pancreatic beta-cell death. *Endocrinology.* **144:** 4154–4163.
36. Mishra, R., and M. S. Simonson. 2005. Saturated free fatty acids and apoptosis in microvascular mesangial cells: palmitate activates pro-apoptotic signaling involving caspase 9 and mitochondrial release of endonuclease G. *Cardiovasc. Diabetol.* **4:** 2.
37. Oakes, N. D., A. Kjellstedt, G. B. Forsberg, T. Clementz, G. Camejo, S. M. Furler, E. W. Kraegen, M. Olwegard-Halvarsson, A. B. Jenkins, and B. Ljung. 1999. Development and initial evaluation of a novel method for assessing tissue-specific plasma free fatty acid utilization in vivo using (R)-2-bromopalmitate tracer. *J. Lipid Res.* **40:** 1155–1169.
38. Xue, X., J. H. Piao, A. Nakajima, S. Sakon-Komazawa, Y. Kojima, K. Mori, H. Yagita, K. Okumura, H. Harding, and H. Nakano. 2005. Tumor necrosis factor alpha (TNFalpha) induces the unfolded protein response (UPR) in a reactive oxygen species (ROS)-dependent fashion, and the UPR counteracts ROS accumulation by TNFalpha. *J. Biol. Chem.* **280:** 33917–33925.
39. Karaskov, E., C. Scott, L. Zhang, T. Teodoro, M. Ravazzola, and A. Volchuk. 2006. Chronic palmitate but not oleate exposure induces endoplasmic reticulum stress, which may contribute to INS-1 pancreatic beta-cell apoptosis. *Endocrinology.* **147:** 3398–3407.

40. Zhivotovsky, B., A. Samali, A. Gahm, and S. Orrenius. 1999. Caspases: their intracellular localization and translocation during apoptosis. *Cell Death Differ.* **6:** 644–651.
41. Rao, R. V., E. Hermel, S. Castro-Obregon, G. del Rio, L. M. Ellerby, H. M. Ellerby, and D. E. Bredesen. 2001. Coupling endoplasmic reticulum stress to the cell death program. Mechanism of caspase activation. *J. Biol. Chem.* **276:** 33869–33874.
42. Xu, C., B. Bailly-Maitre, and J. C. Reed. 2005. Endoplasmic reticulum stress: cell life and death decisions. *J. Clin. Invest.* **115:** 2656–2664.
43. Hotamisligil, G. S. 2005. Role of endoplasmic reticulum stress and c-Jun NH2-terminal kinase pathways in inflammation and origin of obesity and diabetes. *Diabetes.* **54 (Suppl.):** 73–78.
44. Kaneto, H., T. A. Matsuoka, Y. Nakatani, D. Kawamori, T. Miyatsuka, M. Matsuhisa, and Y. Yamasaki. 2005. Oxidative stress, ER stress, and the JNK pathway in type 2 diabetes. *J. Mol. Med.* **83:** 429–439.
45. Wang, D., Y. Wei, and M. J. Pagliassotti. 2006. Saturated fatty acids promote endoplasmic reticulum stress and liver injury in rats with hepatic steatosis. *Endocrinology.* **147:** 943–951.
46. Hickson-Bick, D. L., M. L. Buja, and J. B. McMillin. 2000. Palmitate-mediated alterations in the fatty acid metabolism of rat neonatal cardiac myocytes. *J. Mol. Cell. Cardiol.* **32:** 511–519.
47. Miller, T. A., N. K. LeBrasseur, G. M. Cote, M. P. Trucillo, D. R. Pimentel, Y. Ido, N. B. Ruderman, and D. B. Sawyer. 2005. Oleate prevents palmitate-induced cytotoxic stress in cardiac myocytes. *Biochem. Biophys. Res. Commun.* **336:** 309–315.
48. Feng, B., P. M. Yao, Y. Li, C. M. Devlin, D. Zhang, H. P. Harding, M. Sweeney, J. X. Rong, G. Kuriakose, E. A. Fisher, et al. 2003. The endoplasmic reticulum is the site of cholesterol-induced cytotoxicity in macrophages. *Nat. Cell Biol.* **5:** 781–792.
49. Li, Y., M. Ge, L. Ciani, G. Kuriakose, E. J. Westover, M. Dura, D. F. Covey, J. H. Freed, F. R. Maxfield, J. Lytton, et al. 2004. Enrichment of endoplasmic reticulum with cholesterol inhibits sarcoplasmic-endoplasmic reticulum calcium ATPase-2b activity in parallel with increased order of membrane lipids: implications for depletion of endoplasmic reticulum calcium stores and apoptosis in cholesterol-loaded macrophages. *J. Biol. Chem.* **279:** 37030–37039.
50. Newmeyer, D. D., and S. Ferguson-Miller. 2003. Mitochondria: releasing power for life and unleashing the machineries of death. *Cell.* **112:** 481–490.
51. Semenov, D. V., P. A. Aronov, E. V. Kuligina, M. O. Potapenko, and V. A. Richter. 2004. Oligonucleosome DNA fragmentation of caspase 3 deficient MCF-7 cells in palmitate-induced apoptosis. *Nucleosides Nucleotides Nucleic Acids.* **23:** 831–836.
52. Dowhan, W. 1997. Molecular basis for membrane phospholipid diversity: why are there so many lipids? *Annu. Rev. Biochem.* **66:** 199–232.
53. Cornelius, F. 2001. Modulation of Na,K-ATPase and Na-ATPase activity by phospholipids and cholesterol. I. Steady-state kinetics. *Biochemistry.* **40:** 8842–8851.
54. Allende, D., A. Vidal, and T. J. McIntosh. 2004. Jumping to rafts: gatekeeper role of bilayer elasticity. *Trends Biochem. Sci.* **29:** 325–330.
55. Devries-Seimon, T., Y. Li, P. M. Yao, E. Stone, Y. Wang, R. J. Davis, R. Flavell, and I. Tabas. 2005. Cholesterol-induced macrophage apoptosis requires ER stress pathways and engagement of the type A scavenger receptor. *J. Cell Biol.* **171:** 61–73.